Optimal disturbance rejection for PI controller with constraints on relative delay margin

Article *in* ISA Transactions · March 2016

DOI: 10.1016/j.isatra.2016.03.014

3 authors, including:

Li Sun

Tsinghua University

18 PUBLICATIONS **24** CITATIONS

ISA Transactions ■ (■■■■) ■■■–■■■

Contents lists available at ScienceDirect

ISA Transactions

journal homepage: www.elsevier.com/locate/isatrans

Research Article

Optimal disturbance rejection for PI controller with constraints on relative delay margin

Li Sun [a,*], Donghai Li [a], Kwang Y. Lee [b]

[a] State Key Lab of Power Systems, Department of Thermal Engineering, Tsinghua University, Beijing 100084, PR China
[b] Department of Electrical and Computer Engineering, Baylor University, Waco, TX 76798, USA

ARTICLE INFO

Article history:
Received 17 May 2015
Received in revised form
16 March 2016
Accepted 16 March 2016
This paper was recommended for publication by Dong Lili.

Keywords:
Disturbance rejection
Relative delay margin
PI tuning
Robustness constrained optimization

ABSTRACT

Performance optimization with robustness constraints is frequently encountered in process control. Motivated by the analytical difficulties in dealing with the conventional robustness index, e.g., maximum sensitivity, we introduce the relative delay margin as a good alternative, which gives much simpler robust analysis. This point is illustrated by designing an optimal PI controller for the first-order-plus-dead-time (FOPDT) model. It is first shown that the PI controller parameters can be analytically derived in terms of a new pair of parameters, i.e., the phase margin and gain crossover frequency. The stability region of PI controller is subsequently obtained with a much simpler procedure than the existing approaches. It is further shown that a certain relative delay margin can represent the robustness level well and the contour can be sketched with a simpler procedure than the one using maximum sensitivity index. With constraints on the relative delay margin, an optimal disturbance rejection problem is then formulated and analytically solved. Simulation results show that the performance of the proposed methodology is better than that of other PI tuning rules. In this paper, the relative delay margin is shown as a promising robustness measure to the analysis and design of other advanced controllers.

1. Introduction

In spite of the flourishing of the advanced control theory over the past 60 years, the Proportional-Integral-Derivative (PID) controller still bears the largest workload and undoubtedly plays the dominant role in the current industrial processes. Fig. 1 shows a new survey conducted in more than 100 boiler-turbine units in Guangdong Province, China. Each unit has 20 to 30 pairs of industrial computers, containing more than 170 feedback loops. It is seen that the single-loop PI controller is dominant in power industry. The derivative control only appears in a few temperature control loops. Moreover, most of the controllers are used in the regulatory mode, confirming that disturbance rejection is the primary concern in process industry [1].

In academia, stability analysis and parameter tuning of PI controller are of great interest. The rigorous stability equations of PI/PID controller are given in [2,3] based on Hermite–Biehler Theorem that is applicable to quasi-polynomials. But the complexity is inappropriate for process engineers. The earliest tuning formula of PI/PID controller dates back to the work by Ziegler and Nicholas [4] in 1942. The original Ziegler and Nicholas (Z–N) method only requires the process information of the ultimate frequency and ultimate gain in a single point where the Nyquist curve intersects the negative real axes (at point 'A' in Fig. 2). The resulting Z–N tuning formula, obtained by direct experiments on the process with some empirical rules, is lack of robustness, particularly for the delay dominated processes [5]. To improve robustness, Åström and Hägglund [6] proposed a dual-point method, i.e., specifying gain margin (g_m) at point 'A' and phase margin (φ_m) at point 'C' in Fig. 2. But the controller parameters in terms of gain and phase margins (GPM) are normally obtained by graphical trial and error, which makes it difficult for practitioners. Ho and Hang [7] derived an analytical tuning formula for the first-order-plus-time-delay (FOPDT) model with $g_m = 3$ and $\varphi_m = 60^\circ$. This setting can result in very good tracking performance and is robust. But the system response to disturbance input is sluggish for lag-dominated processes. Also, since there are two robustness measures, which are gain margin and phase margins, it is not explicit how to alter them to achieve different robustness levels.

Along with the rapid development of robust control in 1990s, Åström and Panagopoulos [8] found that the maximum sensitivity function, M_S, can be a good single robustness measure and integral gain can be a good performance index for disturbance rejection. The robustness constraint can be satisfied by specifying the

* Corresponding author.
E-mail address: sunli12@mails.tsinghua.edu.cn (L. Sun).

http://dx.doi.org/10.1016/j.isatra.2016.03.014
0019-0578/

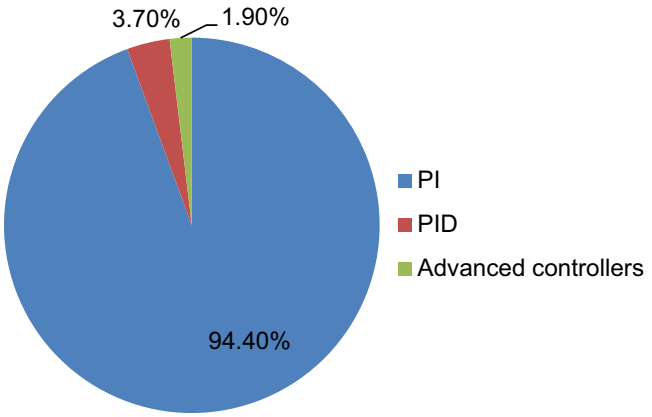

Fig. 1. Distribution of controllers in Power Plants in Guangdong Province, China.

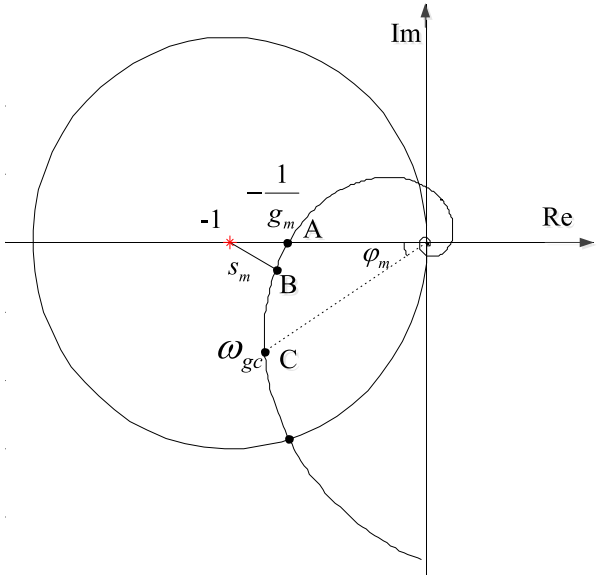

Fig. 2. A typical Nyquist plot of a process, or a process in series with a controller.

shortest distance s_m from the critical point to the Nyquist curve (point 'B' in Fig. 2). The design is based on non-convex optimization, which is later called as M_S-constrained integral gain optimization (MIGO) [9]. In spite of its effectiveness, the computation requirement limits its wide application. By applying the MIGO method with $M_s = 1.4$ to a test batch [9], a curve fitting based tuning formula is obtained for FOPDT model, namely Approximate MIGO (AMIGO). A shortcoming of AMIGO is that it may give a more conservative result compared with MIGO. In this paper, our focus is on the single point 'C' at the gain crossover frequencyw_{gc}, which will lead to a simple analytical solution. The proposed method is an open-loop approach and will be compared with the closed-loop based tuning methods [10–12].

The remainder of the paper is organized as follows: The problem is formulated in Section 2. In Section 3, a simple PI tuning formula and stability regions are derived. The optimization problem constrained by relative delay margin is proposed and solved analytically in Section 4. In Section 5, comparative examples show the merits of the proposed strategy. Main contributions are concluded in Section 6.

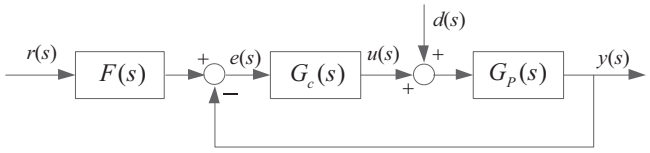

Fig. 3. Structure of a 2-DOF PID/PI system.

2. Backgrounds and problem formulation

2.1. The basic structure

To derive the PI tuning formula for the FOPDT model, we consider the conventional structure of a two degrees of freedom (2-DOF) control system, as shown in Fig. 3. The process model is

$$G_P(s) = \frac{K}{1+Ts} e^{-Ls} \tag{1}$$

where K is the process gain, T the time constant and L the time delay. For a stable process, K, T and L are positive values.

The process is controlled by a 2-DOF PI controller, whose output is expressed as

$$u(t) = k_p \left[(br - y) + \frac{1}{T_i} \int_0^t (r - y) dt \right] \tag{2}$$

where k_p is the proportional gain, T_i the integral time, r, y, d and e are the reference, process output, load disturbance and control error, respectively. Different from the conventional 1-DOF PI, the controller's set-point r is multiplied by a weighting factor b, which can reduce the impact of a step change in the reference and thus reduces the tracking overshoot. In [13], a similar weighting parameter, named rotator factor, is used in discrete-time predictive control. The control law (2) can also be expressed in Laplace domain, as shown in Fig. 3 which consists of a set-point prefilter given by

$$F(s) = \frac{bT_i s + 1}{T_i s + 1} \tag{3}$$

and a feedback controller

$$G_c(s) = k_p \left(1 + \frac{1}{T_i s} \right) \tag{4}$$

Note that the set-point weighting factor b, or the prefilter $F(s)$, only influences the tracking performance, and the disturbance rejection depends solely on the conventional controller $G_c(s)$. In this sense, the objectives of tracking and disturbance rejection can be fulfilled individually in two decoupled steps. One can first design $G_c(s)$ for an optimal disturbance rejection and then use the set-point weighting to smooth the tracking performance. This is the reason why the control law is deemed as 2-DOF.

2.2. Problem formulation

In the past 60 years, optimization has been a major theme in control [14]. For PID tuning, Zhuang and Atherton [15] fitted a series of tuning formulas for FOPDT by minimizing various time weighted integral squared error (ISE) criteria. Li and Xue [16] found that the optimization with integral of time-weighted absolute error (ITAE) criteria can also provide an acceptable robustness. Shinskey [17] formulates an optimization problem with a prescribed robustness for which the problem is addressed in the following form:

Min performance criterion

Subject to robustness limits (5)

Please cite this article as: Sun L, et al. Optimal disturbance rejection for PI controller with constraints on relative delay margin. ISA Transactions (2016), http://dx.doi.org/10.1016/j.isatra.2016.03.014

Along this line, a big step was made by Åström and Persson in [8], where the performance criterion is chosen as the integral error (IE) of the control error in response to the disturbance input. It is further revealed that,

$$\mathrm{IE}=\int_0^\infty [r(t)-y(t)]dt=\frac{T_i}{k_p}=\frac{1}{k_i} \tag{6}$$

for a stable closed-loop system with zero initial error and a unit step load disturbance [5].

Note that (6) is established for disturbance rejection and does not hold for set-point tracking. The robustness index is chosen as the maximum sensitivity function, and is defined as

$$M_s=\max_\omega |S(i\omega)|=\max_\omega \left|\frac{1}{1+G_P(i\omega)G_c(i\omega)}\right| \tag{7}$$

which is the reciprocal of the *stability margin* ([5], see s_m in Fig. 2). The reasonable value of M_s is 1.2–2.0.

Since the work in [8], M_S became the dominant robustness index in literatures on controller tuning. Since the $M_S$constrained optimization is a semi-finite programming problem, which cannot be solved using gradient-based analytical algorithm, Åström and Panagopoulos [8] reduced the semi-finite constraints to a contour of numerous ellipses in the complex plane. The peak of the contour is determined by solving many complicated equations. Another attempt for reducing the computation complexity is made in [18], where M_s is fitted as a high-order polynomial in terms of scaled parameters, so that (5) can be solved by nonlinear programming. Heuristic method is also used in [14] to obtain an optimal solution. There are at least three disadvantages of these methods: (i) risk of local minima of the object function, (ii) huge amount of computation, and (iii) the complicated tuning formula.

2.3. Relative delay margin

Motivated by analytical difficulties in handling the maximum sensitivity function M_S, we seek a new index that can well represent the robustness. And the ratio between the phase margin φ_m and ω_{gc} is called the *delay margin* [19], which represents the allowable largest delay variation such that the closed-loop stability holds. In this paper, the *relative delay margin* will be used as a robustness index, which is defined as

$$R_{dm}=\frac{\varphi_m}{\omega_{gc}L} \tag{8}$$

where L is the time delay of the FOPDT model (1).

The **motivations** to choose R_{dm} as the new robustness measure are given as follows:

(1) The maximum sensitivity function M_S is defined in the closed-loop form, which contains exponential term in the denominator, leading to difficulties in analysis. Additional difficulty comes from the fact that $M_S$is a maximum value over the whole frequency range. On the contrary, R_{dm} is an open-loop measure and all required information for calculation is located in the single point 'C' in Fig. 2.
(2) Many advanced control algorithms can deal well with processes with strong uncertainty and constant delay, but is very sensitive to the variation in the time delay. In [20], only the delay uncertainty is considered for the H_∞ loop shaping and a good robust performance is obtained.
(3) Relative delay margin (8) is dimensionless, whose numerator represents the robustness while the denominator ω_{gc} is closely related to the performance index, i.e., the closed-loop bandwidth.
(4) As is well known, there is a fundamental limit [5] on ω_{gc} for the processes with time delay, i.e.,$\omega_{gc}L<1$. Here, this qualitative inequality is extended for a quantitative purpose.

3. PI tuning formula and stability region

In this section, it is attempted to transform the PI controller parameters into the denominator and numerator of the relative delay margin R_{dm}, which are, φ_m and $\omega_{gc}L$. Both of them are hidden in point 'C' in Fig. 2. Later the stability region of φ_m and $\omega_{gc}L$ are derived, and the stability region of the original parameters (proportional gain k_p and integral gain k_i) can be subsequently obtained.

3.1. Formula derivation in terms of the new pair

By specifying the location of 'C' in Fig. 2, it is possible to obtain two controller parameters as shown below.

With the process G_P in (1) and the controller G_c in (4), the loop transfer function becomes

$$G_L(i\omega)=\left(k_p+\frac{k_i}{i\omega}\right)\left(\frac{K}{1+iT\omega}e^{-i\omega L}\right) \tag{9}$$

Note that the Point 'C' can be denoted as

$$x_c=-\cos(\varphi_m)-i\sin(\varphi_m) \tag{10}$$

Unlike the polar form in the GPM design, here (9) can be expanded in a rectangular form:

$$G_L(i\omega)=\mathrm{Re}(\omega)+i\mathrm{Im}(\omega) \tag{11}$$

where

$$\mathrm{Re}(\omega)=Kk_p\frac{\cos(L\omega)-T\omega\sin(L\omega)}{T^2\omega^2+1}-Kk_i\frac{\sin(L\omega)+T\omega\cos(L\omega)}{\omega\left(T^2\omega^2+1\right)} \tag{12}$$

$$\mathrm{Im}(\omega)=-Kk_p\frac{\sin(L\omega)+T\omega\cos(L\omega)}{T^2\omega^2+1}-Kk_i\frac{\cos(L\omega)-T\omega\sin(L\omega)}{\omega\left(T^2\omega^2+1\right)} \tag{13}$$

Note that the real and imaginary parts are both linear combinations of k_p and k_i. It is thus possible to obtain the analytical solution of the controller parameters by equating (10) and (11) at point 'C':

$$\begin{cases} Kk_p\frac{L(\cos(a)-Ta\sin(a))}{L^2+T^2a^2}-Kk_i\frac{L^2(\sin(a)+Ta\cos(a))}{a(L^2+T^2a^2)}=-\cos(\varphi_m) \\ -Kk_p\frac{L(\sin(a)+Ta\cos(a))}{L^2+T^2a^2}-Kk_i\frac{L^2(\cos(a)-Ta\sin(a))}{a(L^2+T^2a^2)}=-\sin(\varphi_m) \end{cases} \tag{14}$$

where, for simplicity, a dimensionless parameter is used as $a=\omega L$.

After triangular transforms, the following controller parameters are obtained:

$$\begin{cases} k_pK=\frac{T}{L}a\sin(\varphi_m+a)-\cos(\varphi_m+a) \\ k_iKL=a\sin(\varphi_m+a)+\frac{T}{L}a^2\cos(\varphi_m+a) \end{cases} \tag{15}$$

And the integral time of the PI controller is

$$\frac{T_i}{L}=\frac{aT\tan(\varphi_m+a)-L}{aL\tan(\varphi_m+a)+a^2T} \tag{16}$$

As shown in (15) and (16), the simplicity and elegance of the resulting tuning formula is beyond one's expectation. In the conventional combination of gain and phase margins, no such simple equations can be obtained even with approximations.

Based on (15) and (16), some insights are given as below:

1) It is wise to choose the process gain K and time delay L as scaling factors, which makes the ratio of the lag time T and time delay L explicitly shown in the tuning formulae.

Please cite this article as: Sun L, et al. Optimal disturbance rejection for PI controller with constraints on relative delay margin. ISA Transactions (2016), http://dx.doi.org/10.1016/j.isatra.2016.03.014

2) Decreasing φ_m or increasing a corresponds to a larger k_i, which may lead to an improved disturbance rejection but a poor robustness.
3) For lag-dominant processes (large T/L), k_i is determined by $a^2 \cos(\varphi_m+a)$. That is, a large φ_m is not preferable for disturbance rejection.
4) For delay-dominant processes (small T/L), k_i is mainly influenced by $a \sin(\varphi_m+a)$. That is, the φ_m+a close to $\pi/2$ will be good for disturbance rejection.

3.2. Closed-loop stability analysis in terms of φ_m and a

To obtain the stable region of PI controller, Shefiei and Shenton [21] proposed a search method by scanning the frequency ω from 0 to ∞. Silva and Datta [2,3] derived a set of analytical equations describing the stability region based on the Hermite–Biehler Theorem, dealing with the infinite number of roots of quasi-polynomials with the time-delay term. In this section, it will be shown that it is simpler to obtain the stable region under the new space of φ_m and a.

Before the derivation, it should be noted that a is not only the denominator of R_{dm}, but also the phase lag contributed by the time delay e^{-Ls}. Also, the phase lag of $1/(1+Ts)$ can be expressed as $\tan^{-1}(aT/L)$. We now have the following stability conditions:

Lemma 1. *The inequity $k_i \geq 0$ is a necessary condition of the stability of the control system.*

Proof. The closed-loop transfer function of the control system (see Fig. 3) consisting of the process (1) and the controller (4) is

$$G_{CL}=\frac{G_C G_p}{1+G_C G_p}=\frac{\left(k_p+\frac{k_i}{s}\right)\frac{K}{1+Ts}e^{-Ls}}{1+\left(k_p+\frac{k_i}{s}\right)\frac{K}{1+Ts}e^{-Ls}}=\frac{Kk_p s+Kk_i}{(1+Ts)se^{Ls}+Kk_p s+Kk_i} \tag{17}$$

The characteristic equation $\delta(s)$ is a quasi-polynomial which is given by

$$\delta(s)=(1+Ts)se^{Ls}+Kk_p s+Kk_i \tag{18}$$

Evidently, $\delta(s)$ will have positive roots in the case of $k_i<0$. Thus we choose $k_i \geq 0$. □

Theorem 1. *The closed-loop stability of the PI control system holds if and only if*

$$\varphi_m \geq 0,\ \ a \geq 0,\ \ a+tan^{-1}\left(\frac{aT}{L}\right)+\varphi_m \leq \pi \tag{19}$$

Proof. By definition, $a \geq 0$.

Necessity: The inequity $\varphi_m \geq 0$ can be obtained easily from the stability condition. Due to the stability, $k_i \geq 0$ from Lemma 1. According to (15), for $k_i=0$,

$$a=0 \text{ or } \tan(\varphi_m+a)=-\frac{T}{L}a; \tag{20}$$

For $k_i>0$,

$$0 \leq (\varphi_m+a) \leq \frac{\pi}{2} \tag{21}$$

can satisfy the condition. For $k_i>0$ and $(\varphi_m+a)>\frac{\pi}{2}$,

$$a \sin(\varphi_m+a)+\frac{T}{L}a^2 \cos(\varphi_m+a)>0 \tag{22}$$

$$\tan(\varphi_m+a)<-\frac{T}{L}a \tag{23}$$

Finally, from (20) through(23), we can conclude that

$$\varphi_m \geq 0,\ \ a \geq 0,\ \ a+\varphi_m+\tan^{-1}\left(\frac{aT}{L}\right) \leq \pi \tag{24}$$

Sufficiency: Here the closed-loop stability will be proved based on (19). Denoting the phase lag of PI controller at the gain crossover frequency as φ_c, we have

$$\tan(\varphi_c)=\frac{k_i}{\omega_{gc}k_p}=\frac{L}{aT_i} \tag{25}$$

Recalling (16), one can rewrite (25) as

$$\tan(\varphi_c)=\frac{L}{aT_i}=\frac{L\ \tan(\varphi_m+a)+aT}{aT\ \tan(\varphi_m+a)-L} \tag{26}$$

Note that the phase lag at the gain crossover frequency contributed by the inertia part, $1/(1+Ts)$, is

$$\varphi_i=\tan^{-1}(\omega_{gc}T)=\tan^{-1}\left(\frac{aT}{L}\right) \tag{27}$$

So (26) can be further simplified as

$$\tan(\varphi_c)=\frac{L\ \tan(\varphi_m+a)+aT}{aT\ \tan(\varphi_m+a)-L}=-\frac{\tan(\varphi_m+a)+\ \tan(\varphi_i)}{1-\ \tan(\varphi_i)\tan(\varphi_m+a)}$$
$$=-\ \tan(\varphi_m+a+\varphi_i) \tag{28}$$

implying that

$$\varphi_c=\pi-(\varphi_m+a+\varphi_i). \tag{29}$$

Note that $0 \leq \varphi_c \leq \frac{\pi}{2}$ for $k_p \geq 0$ and $\frac{\pi}{2}<\varphi_c \leq \pi$ for $k_p<0$. Thus, it can be concluded that the possible values of the phase lag provided by the PI controller are within the range,

$$0 \leq \varphi_c \leq \pi \tag{30}$$

Thus, for a given $\varphi_m \geq 0$ and the upper bound of the bandwidth a, given by the inequality

$$a+\tan^{-1}\left(\frac{aT}{L}\right)+\varphi_m \leq \pi \tag{31}$$

the controller can be realized and the closed-loop stability can be guaranteed according to the Nyquist open-loop stability criterion. □

The bandwidth beyond this range will lead to an unattainable φ_c, which cannot be provided by the controller even though $\varphi_m \geq 0$. Note that a large bandwidth beyond this range will result in a negative k_i.

Also, (19) can be considered as a general extension of the empirical rule, $\omega_{gc}L<1$. Now the stability region of φ_m and a has already been obtained. Thus the corresponding stability region of k_p and k_i can be further drawn by mapping the contour of φ_m and a based on (15).

3.3. Stability region of k_p and k_i

In order to determine the stability region of the original controller parameters k_p and k_i, a multivariable constrained nonlinear optimization problem should be formulated based on (15) and (19), which are generally solved according to the Karush–Kuhn–Tucker (KKT) condition. But the KKT method needs sophisticated derivation and justification. Here a brief but somewhat less rigorous method will be given to determine the stability region in the sense that φ_m equals 0 in the upper boundary of the stability region.

Please cite this article as: Sun L, et al. Optimal disturbance rejection for PI controller with constraints on relative delay margin. ISA Transactions (2016), http://dx.doi.org/10.1016/j.isatra.2016.03.014

Theorem 2. *The range of k_p values for which a given FOPDT plant (1) can be stabilized using a PI controller is given by*

$$-\frac{1}{K}<k_p<\frac{1}{K}\left[\frac{T}{L}\alpha\ \sin(\alpha)-\ \cos(\alpha)\right] \tag{32}$$

where α is the solution of the equation, and

$$\tan(\alpha)=-\frac{T}{L}\alpha \tag{33}$$

in the interval $(\pi/2,\pi)$.

For a given k_p limited by (32), the range of k_i guaranteeing the stability is given by

$$0\le k_i<\frac{z}{KL}\left[\sin(z)+\frac{T}{L}z\ \cos(z)\right] \tag{34}$$

where z is the solution of the equation

$$k_pK+\ \cos(z)-\frac{T}{L}z\ \sin(z)=0 \tag{35}$$

in the interval $(0,\alpha)$.

Proof. From Lemma 1, the lower boundary of the stability region is $k_i=0$, which can be reached by setting $a=0$. By letting $\varphi_m=0$, the expression of the controller parameters in the upper boundary can be obtained as follows

$$\begin{cases} k_p=\frac{1}{K}\left[\frac{T}{L}a\ \sin(a)-\ \cos(a)\right] \\ k_i=\frac{a}{KL}\left[\sin(a)+\frac{T}{L}a\ \cos(a)\right] \end{cases} \tag{36}$$

From (25), the range of a is reduced to

$$a\ge 0,\ \ \tan(a)\le-\frac{T}{L}a \tag{37}$$

Note the αdefined in (33) is actually the upper bounds of a because

$$\frac{d\left[\tan(a)+aT/L\right]}{da}=1+\tan^2(a)+\frac{T}{L}>0 \tag{38}$$

It is necessary to prove the monotonicity of k_p in the interval $[0,\alpha]$. Differentiating k_p with respect to a, we have

$$\begin{aligned}\frac{dk_p}{da}&=\frac{1}{K}\left[\sin(a)+\frac{T\ \sin(a)}{L}+\frac{Ta\ \cos(a)}{L}\right]\\&=\frac{1}{K\ \cos(a)}\left[\tan(a)+\frac{T\ \tan(a)}{L}+\frac{Ta}{L}\right]\end{aligned} \tag{39}$$

From (39), k_p is monotone in terms of a in the interval $[0,\pi/2]$. In the interval $(\pi/2,\ \alpha]$, we have

$$\tan(a)+\frac{T\ \tan(a)}{L}+\frac{Ta}{L}\le-\frac{T}{L}a-\frac{T^2}{L^2}a+\frac{Ta}{L}=-\frac{T^2}{L^2}a\le 0 \tag{40}$$

Since $\cos(a)<0$, it can be concluded that

$$\frac{dk_p}{da}\ge 0 \tag{41}$$

in the interval $[0,\alpha]$. So the lower and upper bound of k_p can be obtained at $a=0$ and $a=\alpha$, respectively. Therefore we have

$$-\frac{1}{K}<k_p<\frac{1}{K}\left[\frac{T}{L}\alpha\ \sin(\alpha)-\ \cos(\alpha)\right] \tag{42}$$

For a given k_p in the boundary of stability region, we can get the corresponding a from (36) by solving

$$k_pK+\ \cos(a)-\frac{T}{L}a\ \sin(a)=0 \tag{43}$$

Due to the monotonicity shown in (41), there will be only one root of (43) in the interval $[0,\alpha]$. The solution can be easily determined by Newton–Raphson method.

Since the solution a of (43) corresponds to the upper boundary of the stability region for a givenk_p, the upper bound of k_i can be thus obtained by substituting a into (36). Recalling Lemma 1, we have the stability range ofk_i,

$$0\le k_i<\frac{a}{KL}\left[\sin(a)+\frac{T}{L}a\ \cos(a)\right] \tag{44}$$

The theorem can be obtained by replacing a with z. □

Based on (33), the upper bound of k_p can also be expressed as

$$\begin{aligned}\tfrac{1}{K}\left[\tfrac{T}{L}\alpha\ \sin(\alpha)-\ \cos(\alpha)\right]&=-\tfrac{1}{K}\left[\tan(\alpha)\sin(\alpha)+\ \cos(\alpha)\right]\\&=-\frac{1}{K\ \cos(\alpha)}\left[\sin^2(\alpha)+\cos^2(\alpha)\right]\\&=-\frac{1}{K\ \cos(\alpha)}==\frac{\sqrt{1+\tan^2(\alpha)}}{K}=\frac{T}{KL}\sqrt{\alpha^2+\frac{T^2}{L^2}}\end{aligned} \tag{45}$$

The (Eqs. (32)-(35) and 45) describing the stability region are exactly same as the ones in [2,3] derived from Hermite–Biehler Theorem.

At last, an example for determining the stability region of a lag-dominated process is given by

$$G_P(s)=\frac{1}{1+15s}e^{-s} \tag{46}$$

The results in terms of φ_m and a are shown in Fig. 4 based on (19). According to (32)–(35), the stable region of k_p and k_i is given in Fig. 5. In addition, the contour of $R_{dm}=1.63$ is also drawn in both figures.

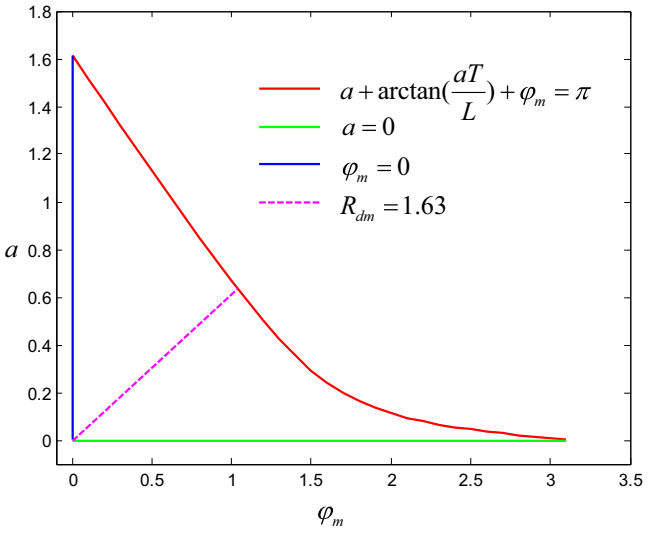

Fig. 4. Stability region in terms of φ_m and a.

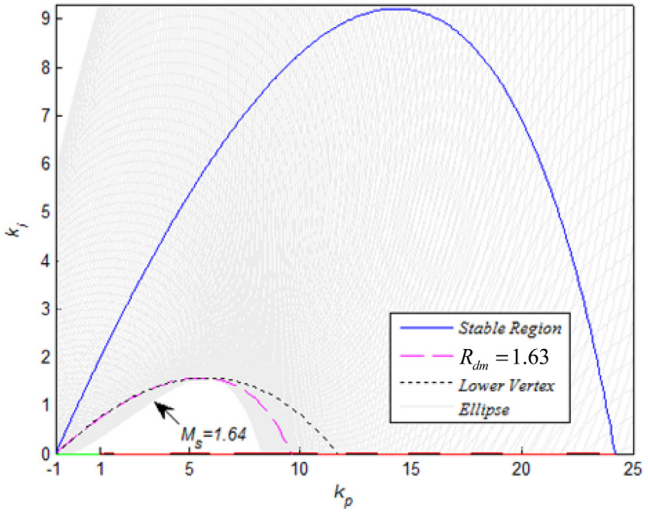

Fig. 5. Stability region of k_p and k_i.

Please cite this article as: Sun L, et al. Optimal disturbance rejection for PI controller with constraints on relative delay margin. ISA Transactions (2016), http://dx.doi.org/10.1016/j.isatra.2016.03.014

Based on the methods proposed in [8], the contour of $M_S = 1.64$ is also given in Fig. 5 by drawing the envelope of numerous ellipses. The lower vertex of the ellipses, which is intended for simply determining the peak, is shown by dotted line. It is surprising to find that the contour of $M_S = 1.64$ shares the same peak, i.e., the same $k_i$and M_S, as that of $R_{dm} = 1.63$. In other words, it implies that the R_{dm} contour may represent a reasonable robustness region. In the next section, we will obtain a reasonable setting of φ_m and a with a simpler constrained optimization procedure.

4. Delay robustness constrained Optimization (DRO tuning)

From the process model (1) and the controller (15), the loop transfer function can be obtained as

$$G_L(\tilde{s}) = \left[\frac{T}{L}a\ \sin(\varphi_m+a) - \cos(\varphi_m+a) + \frac{a\ \sin(\varphi_m+a)+\frac{T}{L}a^2\ \cos(\varphi_m+a)}{\tilde{s}}\right]\frac{K}{1+\frac{T}{L}\tilde{s}}e^{-\tilde{s}} \tag{47}$$

where, $\tilde{s} = Ls$. Evidently, for the processes with a given T/L, the robustness indices, g_m and M_s, will be determined only by φ_m and a. In order to characterize the lag/delay ratio in the whole range, the normalized time delay is defined as

$$\tau = \frac{L}{T+L} \tag{48}$$

where τ is normalized within the range of [0, 1]. Motivated by the phenomenon shown in Fig. 5, we discuss the optimal disturbance rejection constrained by relative delay margin (R_{dm}) under different normalized time delay in this section.

4.1. R_{dm} constrained integral gain optimization

As mentioned in Section 2.2, the integral gain k_i can be considered as a good index of disturbance rejection. Similar to the M_s constrained integral gain optimization (MIGO) [8] method, here the R_{dm} constrained integral gain optimization is formulated as:

$$\max\ a\ \sin(\varphi_m+a)+\tfrac{T}{L}a^2\ \cos(\varphi_m+a)$$
$$s.t.\ R_{dm} = \varphi_m/a = r_{dm} \tag{49}$$

where the objective function is the scaled integral gain (15) in terms of φ_m and a, and r_{dm} is a certain value representing a desired robustness level. This optimization problem can be solved by substituting the constraint into the object function. Then the optimum can be obtained by

$$\frac{d}{da}\left[a\ \sin((r_{dm}+1)a)+\frac{T}{L}a^2\ \cos((r_{dm}+1)a)\right] = 0 \tag{50}$$

which can be further transformed to an algebraic equation,

$$\sin(a(r_{dm}+1))+a\ \cos(a(r_{dm}+1))(r_{dm}+1) + \frac{2Ta\ \cos(a(r_{dm}+1))}{L} - \frac{Ta^2\ \sin(a(r_{dm}+1))(r_{dm}+1)}{L} = 0. \tag{51}$$

The roots of (51) can be numerically obtained in the interval $[0\quad \beta]$. The upper boundβ can be determined from a monotone equation based on (19), which is

$$\beta + \arctan\left(\frac{\beta T}{L}\right) + \beta r_{dm} = \pi \tag{52}$$

Now a and other parameters and indices can be fully determined based on (51), (52) and (15). That is, for a given model with a known normalized time delay τ, the controller parameters, performance and robustness are uniquely dependent on r_{dm}. The distribution of k_i and M_S is shown in Fig. 6 by adjusting r_{dm} from 1 to 3. In addition, some other conventional indices for a certain τ are given in Fig. 7. It is obvious that the robustness is improved with r_{dm} while the performance indices (k_i and a) decrease.

The design procedure described above is named as Delay Robustness based Optimization (DRO), which can also be interpreted as Disturbance Rejection oriented Optimization.

4.2. Recommended parameter setting

Based on numerous results obtained by DRO, Table 1 summarizes a set of recommended parameters in terms of τ, which are mean values of samples selected from four consecutive segments. The selected samples are of quick disturbance response and of no overshoot, (i.e., in this case, IE=IAE). It is found that the tracking performance is quite reasonable with two constant set-point weighting factors while, in other researches, b usually needs to be manually tuned.

5. Illustrative examples

In this section, the efficacy of the DRO method is demonstrated via three simple examples. A commonly used metric, that is, the integrated absolute error (IAE) is given by

$$\mathrm{IAE} = \int_0^\infty |r(t)-y(t)|\ dt \tag{53}$$

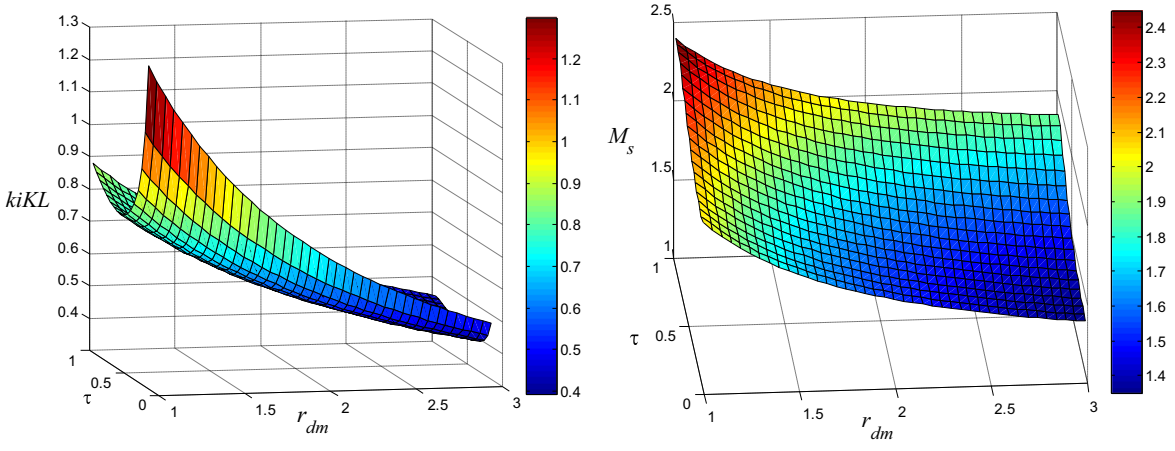

Fig. 6. The distribution of k_i and M_S in terms of τ and r_{dm}.

Please cite this article as: Sun L, et al. Optimal disturbance rejection for PI controller with constraints on relative delay margin. ISA Transactions (2016), http://dx.doi.org/10.1016/j.isatra.2016.03.014

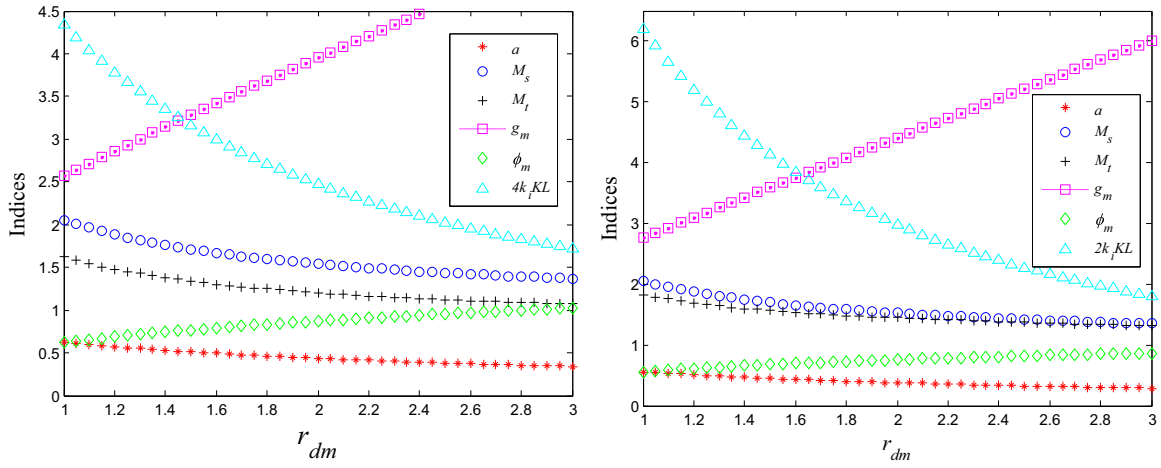

Fig. 7. Performance and robustness indices based on DRO (left: $\tau=0.2$; right: $\tau=0.05$).

Table 1
Recommended settings of DRO tuning.

Parameters	$\tau \le 0.05$	$0.05 \le \tau < 0.1$	$0.1 \le \tau < 0.3$	$\tau \ge 0.3$
φ_m	0.73	0.80	0.94	1.05
a	0.47	0.48	0.50	0.52
b	0.6	0.6	0.6	1

Table 2
PI Controller setting for Example 1.

Method	b	k_p	T_i (min)	M_S	IAEsp	IAE_{ld}
Jin/Liu	0.5	0.83	2.65	1.60	2.54	3.19
AMIGO	1	0.38	2.72	1.23	3.93	7.12
SIMC	1	0.88	3.2	1.59	2.35	3.64
DRO	0.6	0.80	2.41	1.60	2.69	3.01

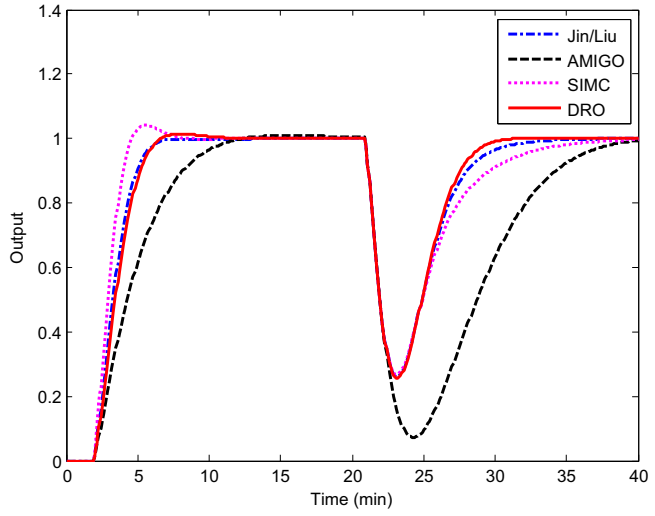

Fig. 8. Servo ($t=1$ min) and regulatory ($t=20$ min) responses in Example 1.

5.1. Example 1. FOPDT Plant

Jin and Liu [15] introduced a FOPDT model for a water tank, which is represented by

$$G_P(s)=\frac{1.895}{(3.201\ \text{min})s+1}e^{-(0.961\ \text{min})s} \tag{54}$$

Based on the closed-loop shaping and model matching approach, an elaborate IMC-PI design was given in [12]. Here it will be compared with the PI setting given by DRO as well as with the well-known SIMC [10] and AMIGO [9]. The DRO parameters are directly obtained by looking up Table 1 with the normalized time delay$\tau=0.23$. The parameters and indices are summarized in Table 2 and the output responses (with unit set-point change at $t=1$ min and a unit load disturbance added to the system at $t=20$ min) are depicted in Fig. 8. Note that the AMIGO formula was originally fitted from extensive samples using the MIGO method under $M_S=1.4$. In this example, it, however, produces a much more conservative result, which is $M_S=1.23$. The disturbance response of SIMC is a little sluggish while it provides a good trade-off between the servo and regulatory modes.

It can be seen from the comparative results that under the same M_S value, the DRO method provides a better load disturbance rejection than Jin and Liu's method while the set-point tracking is also reasonable. Under the similar robustness, another advantage of DRO is its smaller proportional gain, corresponding to a less sensitive response to measurement noise.

5.2. Example 2. Integrating plus time delay process

Integrating Plus Time Delay (IPTD) process can be considered as an extreme case of FOPDT if the inertia time T is infinitely large. Consider the example from [22], we have

$$G_P(s)=\frac{0.2}{s}e^{-7.4s} \tag{55}$$

For DRO tuning, (55) is first approximated with an FOPDT model

$$G_P(s)=\frac{200}{1+1000s}e^{-7.4s} \tag{56}$$

whose normalized time delay is $\tau \le 0.05$Thus the DRO setting is obtained according to the first column in Table 1. To evaluate the proposed method, three latest methods (MoReRT [23], the model matching based method [24] and enhanced IMC-PI by Jin and Liu [22]) are used for comparison. Note that those methods are all derived particularly for the IPTD model whereas the DRO setting is obtained from an approximate FOPDT model.

Table 3 gives the controller settings and performance indices. The output responses are depicted in Fig. 9. It is shown that, compared with the existing methods, the DRO method gives a significant improvement in tracking and disturbance rejection while sacrificing a little bit robustness.

Please cite this article as: Sun L, et al. Optimal disturbance rejection for PI controller with constraints on relative delay margin. ISA Transactions (2016), http://dx.doi.org/10.1016/j.isatra.2016.03.014

Table 3
Controller settings and performance indices for Example 2.

Method	b	k_p	T_i	M_S	g_m	φ_m (deg)	R_{dm}	Set-point tracking		Disturbance rejection	
								Overshoot (%)	IAE	Overshoot (%)	IAE
Jin/Liu	0.429	0.293	52.432	1.60	3.4	46.7	1.80	0	29.99	0	178.95
Alcantara	1	0.338	99.900	1.65	3.0	52.7	1.82	18	29.08	0	293.09
MoReRT	0.516	0.280	46.006	1.60	3.5	44.7	1.77	3	25.61	1	165.03
DRO	0.6	0.290	38.711	1.69	3.3	40.9	1.52	9	24.29	3	134.53

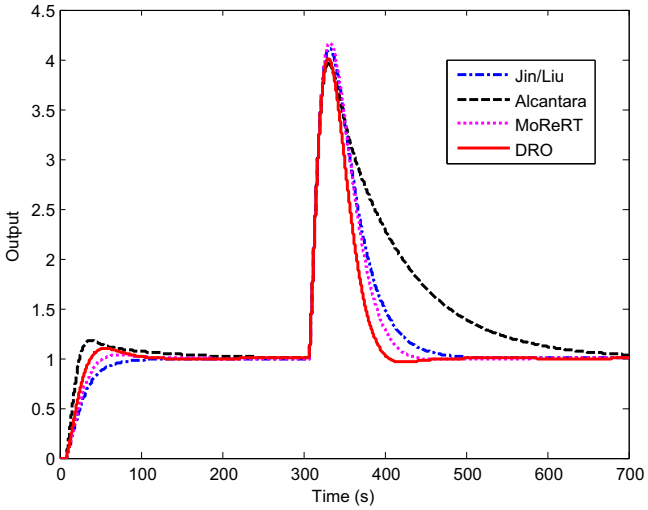

Fig. 9. Responses of servo ($t=1$ s) and regulatory ($t=300$ s) for Example 2.

Table 4
Results of the PI controller for Example 3.

Method	Reduced model	b	k_p	T_i	M_S	IAEsp	IAE_{ld}
AMIGO	$K=1$; $T=2.9$; $L=1.42$	1	0.414	2.66	1.31	6.47	6.41
MoReRT	$K=1$; $T_1=T_2=1.487$; $L=1.11$	0.684	0.731	2.88	1.60	4.90	3.94
SIMC	$K=1$; $T=1.5$; $L=2.5$	1	0.3	1.5	1.46	5.64	5.40
DRO	$K=1$; $T=2.1$; $L=1.9$	0.6	0.54	2.08	1.59	4.98	4.07

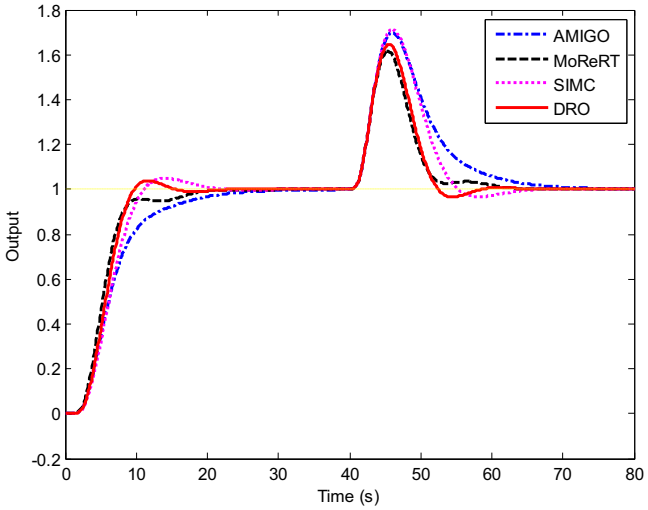

Fig. 10. Servo ($t=1$ s) and regulatory ($t=40$ s) responses in Example 3.

5.3. Example 3. High-order process

Consider a benchmark fourth-order transfer function

$$G_P(s)=\frac{1}{(1+s)^4} \tag{57}$$

For DRO tuning, the model (57) is reduced to a FOPDT model by equaling the magnitude and phase lags to those of FOPDT at the gain crossover frequency ω_{gc}, where the DRO tuning is developed. The model reduction methods of AMIGO [5], MoReRT [11] and SIMC [10] are also used for the corresponding tuning formula. The reduced-order model parameters are listed in Table 4 as well as the controller settings and performance indices. The responses are shown in Fig. 10. Again, the AMIGO method gives a conservative result. The SIMC also shows conservativeness compared with its expected robustness level ($M_S=1.59-1.70$ [10]) because its estimated *delay* is bigger. It is surprising to see that the response of DRO can rival that of MoReRT method because the latter was derived based on the second-order plus time-delay (SOPDT) model. Note that the proportional gain of DRO is again relatively small, compared with other methods under the same robustness level.

6. Conclusion

This paper addresses the adequacy and simplicity of using the relative delay margin as a new robustness measure. The PI tuning formula is analytically derived in terms of the numerator and denominator of relative delay margin. The stability regions for both original and transformed pair of parameters are determined in a simple way. Then a delay robustness constrained optimization (DRO) is formulated and easily solved to tune the controller parameters. For ease of use, a set of recommended parameters is given. Three examples demonstrate that the DRO tuning shows better performance than some recently proposed methods in most cases. Additionally, the proportional gain of DRO is the smallest, compared with other reported methods under the same robustness level, implying that it has the least sensitivity to the noise.

Acknowledgments

Research supported by National Natural Science Foundation of China (No. 51176086). The first author would like to give thanks to the China Scholarship Council (CSC), Grant 201406210142, for funding towards research at Baylor University.

References

[1] Sun L, Dong J, Li D, Lee KY. A practical multivariable control approach based on inverted decoupling and decentralized active disturbance rejection control. Ind Eng Chem Res 2016;55(7):2008–19.
[2] Silva GJ, Datta A, Bhattacharyya SP. New results on the synthesis of PID controllers. IEEE Trans Autom Control 2002;47(2):241–52.

[3] Silva GJ, Datta A, Bhattacharyya SP. PID controllers for time-delay systems. Boston: Springer Science & Business Media; 2005.
[4] Ziegler JG, Nichols NB. Optimum settings for automatic controllers. Trans ASME 1942;64:11.
[5] Åström KJ, Hägglund T. Advanced PID control. NC: ISA – The Instrumentation, Systems, and Automation Society; Research Triangle Park; 2006. p. 27709.
[6] Åström KJ, Hägglund T. Automatic tuning of simple regulators with specifications on phase and amplitude margins. Automatica 1984;20(5):645–51.
[7] Ho WK, Hang CC, Cao LS. Tuning of PID controllers based on gain and phase margin specifications. Automatica 1995;31(3):497–502.
[8] Åström KJ, Panagopoulos H, Hägglund T. Design of PI controllers based on non-convex optimization. Automatica 1998;34:585–601.
[9] Hägglund T, Åström KJ. Revisiting the Ziegler–Nichols tuning rules For PI control. Asian J Control 2002;4(4):364–80.
[10] Skogestad S. Simple analytic rules for model reduction and PID controller tuning. J Process Control 2003;13(4):291–309.
[11] Alfaro VM, Vilanova R. Model-reference robust tuning of 2DoF PI controllers for first- and second-order plus dead-time controlled processes. J Process Control 2012;22(2):359–74.
[12] Jin Qi B, Liu Q. IMC-PID design based on model matching approach and closed-loop shaping. ISA Trans 2014;53(2):462–73.
[13] Zhang B, Yang W, Zong H, Wu Z, Zhang W. A novel predictive control algorithm and robust stability criteria for integrating processes. ISA Trans 2011;50(3):454–60.
[14] Tsien HS. Engineering cybernetics. New York, NY: McGraw-Hill Book Company, Inc; 1954.
[15] Zhuang M, Atherton DP. Automatic tuning of optimum PID controllers. IEE Proc D Control Theory Appl 1993;140(3):216.
[16] Li D, Gao F, Xue Y, Lu C. Optimization of decentralized Pi/Pid controllers based on genetic algorithm. Asian J Control 2007;9(3):306–16.
[17] Shinskey FG. How good are our controllers in absolute performance and robustness? Meas Control 1990;23(4):114–21.
[18] Jin J, Liu Q, Wang Q, Li Q, Wang S, IMC-PID Design Z. Analytical optimization for performance/robustness tradeoff tuning for servo/regulation mode. Asian J Control 2014;16(4):1252–61.
[19] Wang L, Cluett WR. From plant data to process control: ideas for process identification and PID design. New York: Taylor & Francis; 2004.
[20] Zhong QC, Normey-Rico JE. Control of integral processes with dead-time. 1. Disturbance observer-based 2 DOF control scheme. Control Theory Appl IEE Proc 2002;149(4):285–90.
[21] Shafiei Z, Shenton AT. Frequency-domain design of PID controllers for stable and unstable systems with time delay. Automatica 1997;33(12):2223–32.
[22] Jin QB, Liu Q. Analytical IMC-PID design in terms of performance/robustness tradeoff for integrating processes: from 2-Dof to 1-Dof. J Process Control 2014;24(3):22–32.
[23] Alfaro VM, Vilanova R. Robust tuning and performance analysis of 2DoF PI controllers for integrating controlled processes. Ind Eng Chem Res 2012;51(40):13182–94.
[24] Alcántara S, Pedret C, Vilanova R. On the model matching approach to PID design: analytical perspective for robust Servo/Regulator tradeoff tuning. J Process Control 2010;20(5):596–608.

Please cite this article as: Sun L, et al. Optimal disturbance rejection for PI controller with constraints on relative delay margin. ISA Transactions (2016), http://dx.doi.org/10.1016/j.isatra.2016.03.014